The Lattice of the 10 GeV Synchrotron

G. Dugan
LNS, Cornell University

I. ORIGINAL DESIGN LATTICE

The basic geometry of the lattice is defined by the ringwide reference coordinate system, which is a 192-sided polygon[2]. There are 192 equal-strength dipole-gradient magnets in the machine. Each magnet bends the beam through the angle θ, where

$$\theta = \frac{2\pi}{192} = 32.725\,mrad \quad . \tag{1}$$

The reference coordinate system (192-sided polygon) is formed from 192 line segments, each making an angle of θ with the previous segment; the lengths of the line segments are equal to the slot lengths, which are given in table I.

Table I: Synchrotron slot lengths[2]

Lattice element	Slot length(in)	Slot length(m)	Number	Total length(m)
Main dipole	144.98745	3.6826886	186	684.980
Modified dipole	144.98745	3.6826886	6	22.09613
Short straight	240	6.0960	4	24.38405
Long straight	480	12.192	2	24.38405
				755.84423

There are six sectors in the machine. The sectors are separated by short straight sections at L1, L2, L4, and L5, and by long straight sections at L0 and L3. Each sector contains 32 bending magnets. The two magnets on each end of each short straight section are "modified dipoles" used to match the short straights into the rest of the lattice. For the long straights, matching is accomplished by a quadrupole doublet located in the center of the straight section.

The machine lattice is antisymmetric about a line connecting the centers of the L4 and L1 sectors (a sector is named after the upstream straight section, in the electron direction). The focusing arrangement, in the positron direction, starting in the center of the L4 sector (at table 144), is

								H	V	H	V	H	V	H	MV2	L4
MV1	H	V	H	V	H	V	H	V	H	V	H	V	H	V	H	L3
H	V	H	V	H	V	H	V	H	V	H	V	H	V	H	MV2	L2
MV1	H	V	H	V	H	V	H	V	H	V	H	V	H	V	MH2	L1
MH1	V	H	V	H	V	H	V	H	V	H	V	H	V	H	V	L0
V	H	V	H	V	H	V	H	V	H	V	H	V	H	V	MH2	L5
MH1	V	H	V	H	V	H	V									

In the above, H,V,MV1,MV2,MH1,MH2 refer to the following half-cells:

H=HF gradient magnet-VF gradient magnet;
V=VF gradient magnet-HF gradient magnet;
MV2=VF gradient magnet-modified HF gradient magnet;
MV1=modified VF gradient magnet-HF gradient magnet;
MH2=HF gradient magnet- modified VF gradient magnet;
MH1=modified HF gradient magnet-VF gradient magnet;

A. Standard Gradient Magnets

The main synchrotron magnets are combined function gradient dipoles. The pole tip is shaped to produce both a quadrupole and a sextupole component. The horizontally focusing (HF) magnets (called "negative" lenses in the original design report) have a narrow 1.045" gap; the vertically focusing (VF) magnets ("positive" lenses) have a 1.5" gap[1]. The difference in the gaps correlates with the lattice functions to maximize the machine's physical aperture. The HF magnets also contain a 2-turn backleg correction coil winding, although these windings are generally not powered.

The design effective length of the dipole field in the magnets[4] was l=3.238 m. Hence the beam's radius of curvature in the average dipole field is

$$\rho = \frac{l}{2\sin\left[\frac{\theta}{2}\right]} = 98.9504 \ \ m. \tag{2}$$

The average field B as a function of momentum is then

$$B = \frac{10\,p(GeV/c)}{2.998\rho(m)} \ \ T = .033709\,p(GeV/c) \ \ T. \tag{3}$$

At positron injection p=0.2 GeV/c, B=67.4 G; at full energy, p=5.3 GeV/c, B=1787 G.

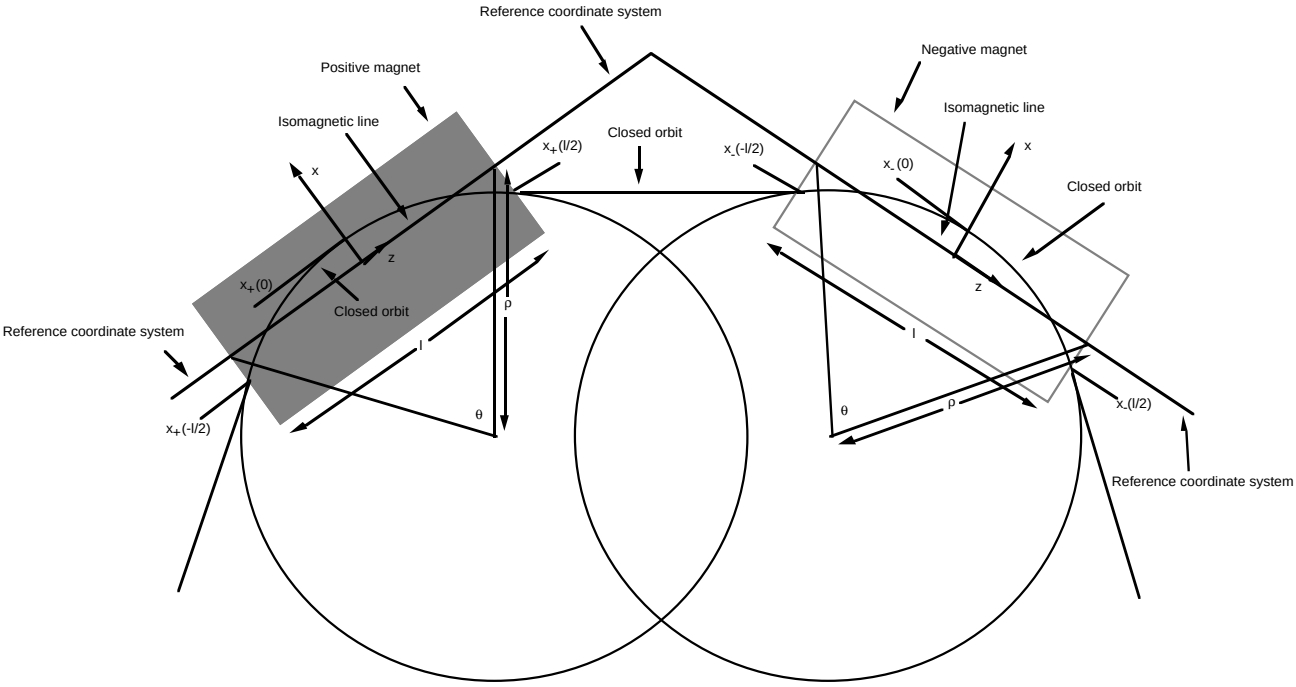

Fig 1: The basic half-cell, showing closed orbit, reference system, and magnets

Fig. 1 shows the closed orbit in the basic half-cell. The heavy black lines in the figure are the line segments of the reference coordinate system associated with these magnets. The "isomagnetic line"[2] is that line along which the field integral along the closed orbit is the same for both the positive and negative magnets.

Ideally, the isomagnetic line for each magnet lies along the reference line segment for that magnet, as shown in Fig. 1. In this case, it is shown in[2] that, for a gradient magnet field of the form

$$B_{\pm}(x) = B_0\left[1 \mp \frac{x}{x_{0\pm}}\right], \tag{4}$$

in which x=0 corresponds to the reference system line, and the gradient length parameter is

$$x_{0\pm} = \mp \frac{B_0}{\frac{dB_{\pm}}{dx}}. \tag{5}$$

the closed orbit has the form

$$\begin{aligned} x_{-}(z) &= -x_{0-} + \frac{\tan\frac{\theta}{2}}{k\sin\left[\frac{kl}{2}\right]}\cos kz \\ x_{+}(z) &= x_{0+} - \frac{\tan\frac{\theta}{2}}{k\sinh\left[\frac{kl}{2}\right]}\cosh kz \end{aligned} \tag{6}$$

in which

$$k^2 = \frac{2\tan\frac{\theta}{2}}{x_0 l} \tag{7}$$

In Eqs. (4) to (6), the negative sign refers to the negative (HF) magnets, the positive sign to the positive (VF) magnets. The average bending field seen by a particle, *B*, is given by

$$B = \frac{1}{2l}\int_{-\frac{l}{2}}^{\frac{l}{2}} dz\left(B_{-}(x_{-}(z)) + B_{+}(x_{+}(z))\right) \tag{7}$$

The result of integrating Eq. (7), using Eq. (6) and (4), is

$$B = B_0 \tag{8}$$

The quadrupole focusing strength parameter, k_1, on the closed orbit, is then

$$k_{1\pm} = \frac{1}{B\rho}\frac{dB_{\pm}}{dx} = \mp\frac{1}{B_0\rho}\frac{B_0}{x_{0\pm}} = \mp\frac{1}{\rho x_{0\pm}}. \tag{8}$$

The original design of the synchrotron lattice[2] specified the values of $x_{0\pm}$, and gradient length, shown in Table II.

Table II: Standard gradient magnet design parameters

Parameter	Positive (VF) wide-gap magnet	Negative(HF) narrow-gap magnet	Unit
Gradient effective length	126.5	126.5	in
x_0	9.145	9.121	in
Quadrupole focusing strength parameter k_1	-.043508	.043622	m^{-2}
ε	.0246	.0173	in^{-1}
Sextupole focusing strength parameter k_2	-.0421376	.029711	m^{-3}

In addition, for chromaticity correction, the magnet design called for an explicit variation of the gradient length x_0 with *x:*

$$x_{0\pm}(x) = \frac{x_{00\pm}}{1 + \varepsilon_{\pm}x}. \tag{9}$$

Using (5), the field is then

$$B_{\pm}(x) = B_0\left[1 \mp \frac{x}{x_{00\pm}}\left(1 + \frac{\varepsilon_{\pm} x}{2}\right)\right]. \tag{10}$$

The sextupole strength parameter k_2 is then

$$k_{2\pm} = \frac{1}{B\rho}\frac{d^2 B_{\pm}}{dx^2} = \mp\frac{1}{B_0\rho}\frac{\varepsilon_{\pm} B_0}{x_{00\pm}} = \mp\frac{\varepsilon_{\pm}}{\rho x_{00\pm}} = \varepsilon_{\pm} k_{1\pm} \tag{11}$$

B. Modified Gradient Magnets

The gradient magnets adjacent to each of the short straight sections were modified in order to match the short straights into the main lattice. The modification was to build the 108.843" of the magnet closest to the straight section with laminations which give a stronger field gradient than the standard gradient magnet. The remaining 17.637" of the magnet contains laminations of the normal strength, but of the opposite gradient. Table III presents the design values for the gradient lengths and focusing strengths for the modified magnets.

Table III: Modified gradient magnet design parameters

Parameter	Positive (MVF) modified wide-gap magnet	Negative(MHF) modified narrow-gap magnet	Unit
Gradient effective length (near straight)	108.863	108.863	in
x_0 (near straight)	4.738	4.731	in
Quadrupole focusing strength parameter k_1 (near straight)	-.0839755	.0840998	m^{-2}
ε (near straight)	.0246	.0173	in^{-1}
Sextupole focusing strength parameter k_1 (near straight)	-.081330	.0572805	m^{-3}
Gradient effective length (away from straight)	17.637	17.637	in
x_0 (away from straight)	9.145	9.121	in
Quadrupole focusing strength parameter k_1 (away from straight)	.043508	-.043622	m^{-2}
ε (away from straight)	.0246	.0173	in^{-1}
Sextupole focusing strength parameter k_1 (away from straight)	.0421376	-.029711	m^{-3}

C. L0 and L3 matching quadrupoles

A quadrupole doublet is used to match each long straight section into the main lattice. The length and placement of the original doublets are given in[1], and are presented in Table IV. The nominal strength of the quadrupoles is also given in [1] as about 5 kG/in. This corresponds to a focusing strength parameter of $k_Q = 0.59$ m^{-2} at 10 GeV. Since this is presumably just a nominal value, and no reference to the original exact design value could be found, the precise design value was determined using a MAD lattice file (see section I.D below) and allowing k_Q to vary to match the lattice functions (β and α only) across the long straight. The value determined in this fashion is shown in Table IV: it differs from the nominal value by about 4%.

Table IV: Synchrotron L0, L3 quadrupole parameters

Parameter	Quadrupole	Unit
Gradient length	.381	m
Quadrupole focusing strength parameter k_Q	.612	m^{-2}
Quadrupole spacing	1.067	m

D. MAD Lattice Calculations

A lattice has been set up with the MAD program according to the information given above. MAD has been run to calculate the lattice functions for comparison with those given in the design report. The global parameters of the design lattice are presented in Table V.

Plots of the lattice functions are given in figs. 2,3, and 4. They agree well with the lattice functions given in [1].

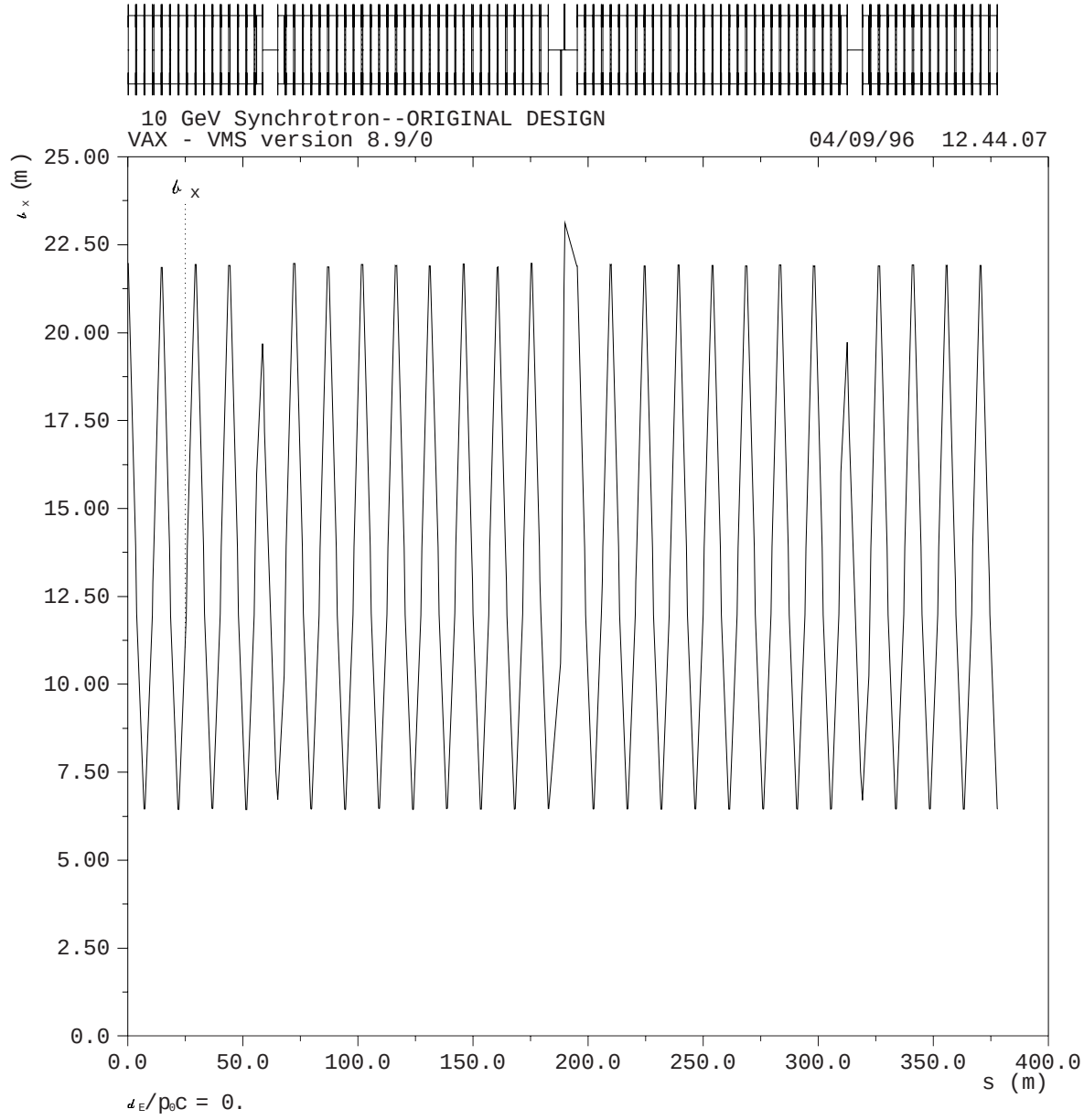

Fig 2.
Original design: horizontal beta function
Half ring, Starting at table 144
in positron direction

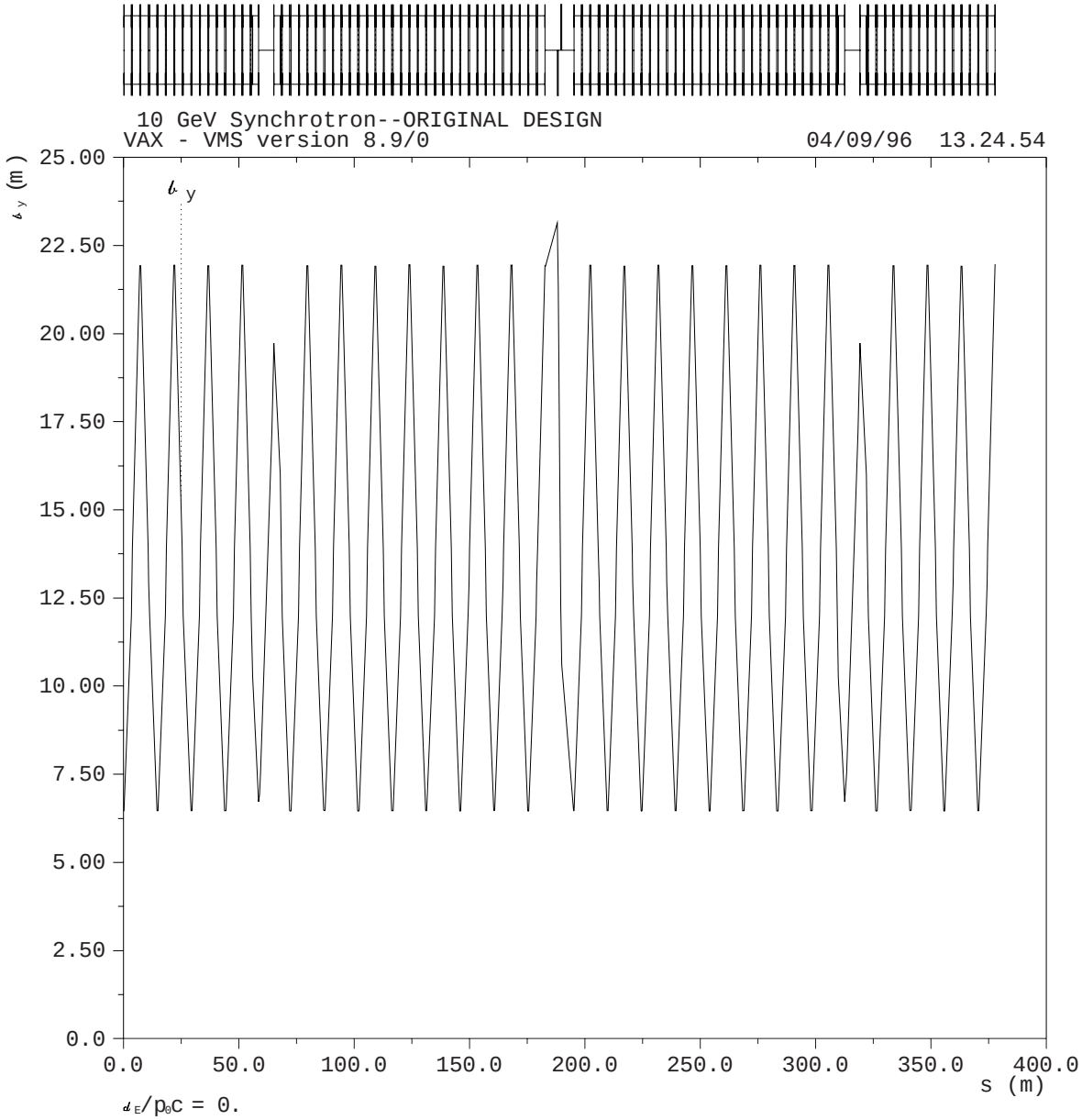

Fig 3.
Original design: vertical beta function
Half ring, Starting at table 144
in positron direction

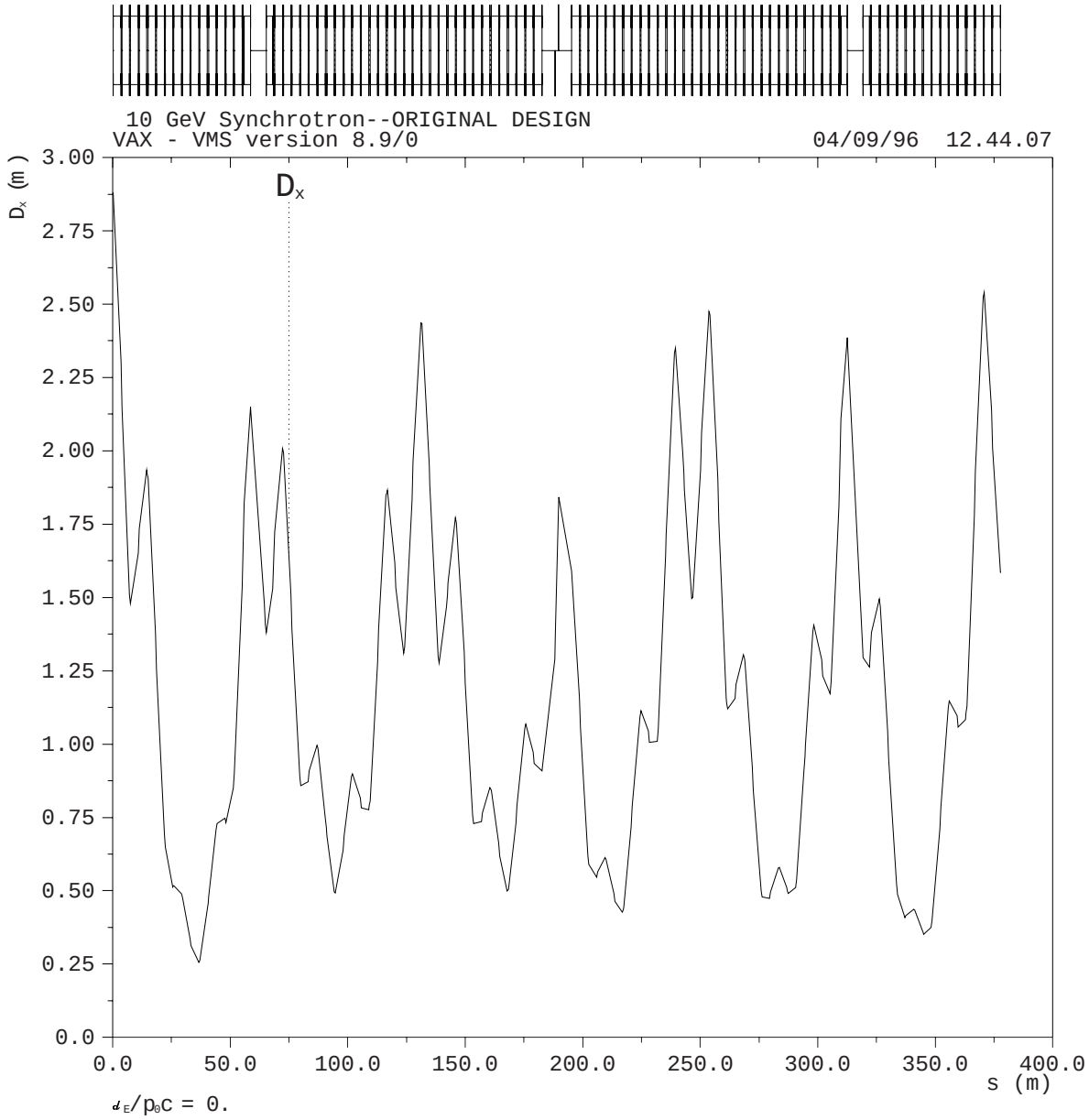

Fig 4.
Original design: horizontal dispersion function
Half ring, Starting at table 144
in positron direction

Table V: Original design global parameters

Parameter	Horizontal	Vertical	Longitudinal	Units
Tune	10.757	10.749		
Chromaticity	-0.623	-1.552		
Momentum compaction			.009588	
Circumference			755.8428	m
Beta(max)	23.11	23.15		m
Dispersion (max)	2.88	0.		

As an overall check, MAD has been asked to vary the standard focusing gradient strengths to obtain a 75.4° phase advance[1] for each cell. The modified magnet focusing gradients have been allowed to vary to obtain a match to the main lattice across the short straights. Consistent with the original design philosophy, the match constraints have not included dispersion. The results are shown in Table VI: MAD verifies the original design choices to high accuracy.

Table VI: Comparison of design focusing parameters vs. optimized MAD focusing parameters

Parameter	Design	MAD	Units	(Design-MAD)/Design
Main HF focusing quadrupole strength	.043622	.043589	m^{-2}	7.6×10^{-4}
Main VF focusing quadrupole strength	-.043508	-.043486	m^{-2}	5×10^{-4}
Modified HF focusing quadrupole strength	.0840998	.0840186	m^{-2}	9.7×10^{-4}
Modified VF focusing quadrupole strength	-.0839755	-.083923	m^{-2}	6.3×10^{-4}

II. PRE-CESR LATTICE

A. Synchrotron Standard-Gradient Field Measurements

From Eqs. (6) above, the closed orbit at the entrance and exit of either type of magnet is

$$x_-(\frac{l}{2}) \approx x_+(\frac{l}{2}) \approx -0.346 \ \ in \tag{12}$$

and at the center it is

$$x_-(0) \approx x_+(0) \approx 0.173 \ \ in. \tag{13}$$

The sagitta is the sum of these numbers, about .52 in. As discussed in [3], if the magnet's magnetic aperture were symmetric about the geometric center, then one would maximize the physical aperture by placing the geometric centerline at

$$x_{center} = 0.5*(-.346+.173) \ \ in = -.0865 \ \ in \tag{14}$$

However, the magnets' good field region is not symmetric about the geometric center, and is not the same for the HF and VF magnets. The HF narrow-gap magnets have a good-field aperture which spans the region from -1.2 in to 1.3 in about the geometric centerline; the VF wide-gap magnets have a good field region from -1. in to 1 in. The result is that the apertures are maximized by choosing for the geometric centerline

$$\begin{aligned} x_{center,-} &= -h_- = -.131 \ \ in \\ x_{center,+} &= -h_+ = -.069 \ \ in \end{aligned} \tag{15}$$

The magnets were designed and measured using a coordinate system centered on the geometric centerline. Using $\xi = x+h$ to denote the transverse coordinate in this system, the magnetic field B' in this system is described in terms of $B'_{0\pm}$, the field at ξ=0, and

$$\xi_{0\pm}(\xi) = \mp \frac{B'_{0\pm}}{\frac{dB'_\pm}{d\xi}} \tag{16}$$

Measured field data[4] are presented as a graph of $\xi_{0\pm}(\xi)$ vs. ξ. To interpret this in modern notation, I define

$$g_{0\pm}(\xi) = \frac{\xi_{00\pm}}{\xi_{0\pm}(\xi)} = \mp \frac{\xi_{00\pm}}{B'_{0\pm}} \frac{dB'_{\pm}}{d\xi} \tag{17}$$

in which $\xi_{00\pm}$ are the *design* values (on the geometric centerline) as given in [3]: ξ_{00-} = 9.01 in, ξ_{00+} = 9.223 in. Then the magnetic field is

$$B'_{\pm}(\xi) = B'_{0\pm}\left[1 \mp \frac{1}{\xi_{00\pm}} \int_0^{\xi} d\xi' g_{0\pm}(\xi')\right]. \tag{18}$$

The standard power series expansion of the field is

$$B'_{\pm}(\xi) = B'_{0\pm} \sum_{n=0} b'_{n\pm} \xi^n \tag{21}$$

If we power series expand g_0,

$$g_{0\pm}(\xi) = \sum_{n=1} g_{n\pm} \xi^{n-1} \tag{22}$$

then we have

$$g_{0\pm}(\xi) = \mp \frac{\xi_{00\pm}}{B'_{0\pm}} \frac{dB'_{\pm}}{d\xi} = \mp \xi_{00\pm} \sum_{n=1} n b'_{n\pm} \xi^{n-1} = \sum_{n=1} g_{n\pm} \xi^{n-1} \tag{23}$$

so the field harmonics are

$$b'_{n\pm} = \mp \frac{g_{n\pm}}{n \xi_{00\pm}} \tag{24}$$

For beam optics, however, we want the field harmonics evaluated on the isomagnetic line, not the geometric centerline. The field expansion about the isomagnetic line is

$$B_{\pm}(x) = B_0 \sum_{n=0} b_{n\pm} x^n \tag{25}$$

Using $\xi = x + h$ in Eq. (21) gives

$$B_{\pm}(x) = B'_{\pm}(x + h_{\pm}) = B'_{0\pm} \sum_{n=0} b'_{n\pm} (x + h_{\pm})^n \tag{26}$$

The field on the isomagnetic line, x=0, is

$$B_{\pm}(0) = B_0 = B'_{\pm}(h_{\pm}) = B'_{0\pm} \sum_{n=0} b'_{n\pm} h_{\pm}^n \tag{27}$$

The focusing strength parameter on the isomagnetic line is then

$$\begin{aligned} k_{n\pm} &= \frac{1}{B\rho} \frac{d^n B_{\pm}}{dx^n}\bigg|_{x=0} = \frac{B'_{0\pm}}{B_0 \rho} \frac{d^n}{dx^n} \sum_{m=1} b'_{m\pm} (x + h_{\pm})^m \bigg|_{x=0} \\ &= \frac{1}{\rho \sum_{m=0} b'_{m\pm} h_{\pm}^m} \frac{d^n}{dx^n} \sum_{m=1} b'_{m\pm} (x + h_{\pm})^m \bigg|_{x=0} \\ &= \mp \frac{\frac{d^n}{dx^n} \sum_{m=1} \frac{g_{m\pm}}{m} (x + h_{\pm})^m \Big|_{x=0}}{\rho \xi_{0\pm} \left[1 \mp \frac{1}{\xi_{00\pm}} \sum_{m=1} \frac{g_{m\pm}}{m} h_{\pm}^m\right]} \end{aligned} \tag{28}$$

The harmonic coefficients in the field expansion about the isomagnetic line, Eq. (25), are related to the focusing strength parameters at x=0 by

$$\begin{aligned} k_{n\pm} &= \frac{1}{B\rho} \frac{d^n B_{\pm}}{dx^n}\bigg|_{x=0} = \frac{n! b_{n\pm}}{\rho} \\ b_{n\pm} &= \frac{\rho k_{n\pm}}{n!} \end{aligned} \tag{29}$$

The data presented in [4] have been fit as described above to obtain the $g_{n\pm}$ coefficients, and from these the focusing strength parameters and the harmonic coefficients on the isomagnetic line have been calculated. The data out to beyond 1 in are well fit with terms up to n=6 in the fit. The fits are shown in figs. 6 and 7.

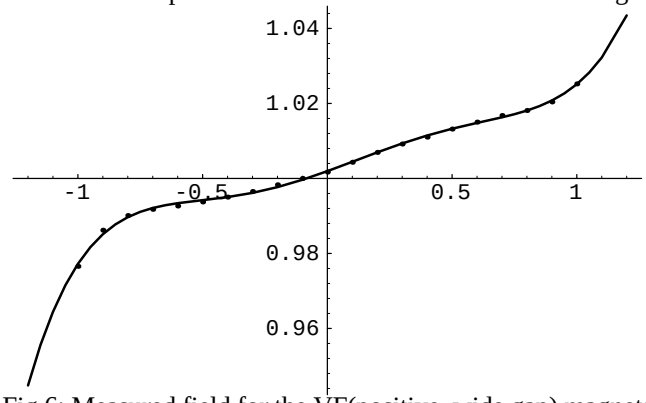

Fig 6: Measured field for the VF(positive, wide gap) magnets
Abscissa: ξ(in); Ordinate: $g_{0+}(\xi)$

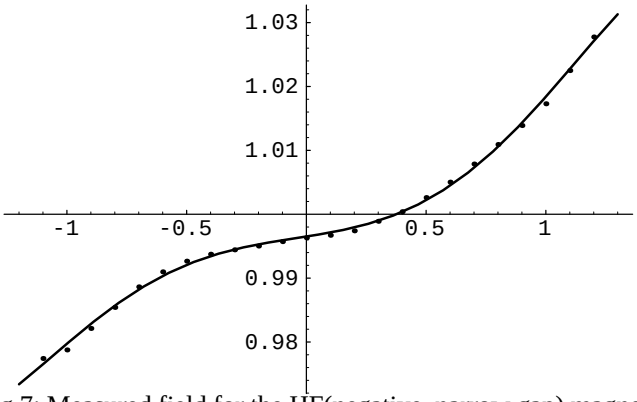

Fig 7: Measured field for the HF(negative, narrow gap) magnets
Abscissa: ξ(in); Ordinate: $g_{0-}(\xi)$

The results are given in Table VII. In computing the focusing strength parameters, the value of ρ appropriate for the *measured* dipole effective length, l(measured)=3.23 m, was used:

$$\rho = \frac{l(measured)}{2sin\left[\frac{\theta}{2}\right]} = 98.7059 \ \ m \tag{30}$$

Table VII: Synchrotron standard magnet measured parameters[4]

Parameter	Positive (VF) wide-gap magnet	Negative(HF) narrow-gap magnet	Unit
Gradient effective length	125.99	126.09	in
g_1	-1.00195	.996514	
g_2	-.024228	.0029436	in^{-1}
g_3	-.009803	.0008122	in^{-2}
g_4	.027557	.004489	in^{-3}
g_5	.0106	.00002212	in^{-4}
g_6	-.02728	-.0007516	in^{-5}
k_1	-.0437352	.0435214	m^{-1}
k_2	-.04319	.012789	m^{-2}
k_3	-.52492	1.27195	m^{-3}
k_4	465.4	275.4	m^{-4}
k_5	2922.	-7153.8	m^{-5}
k_6	-1.34×10^7	-2.2×10^6	m^{-6}
b_1	-1096.4	1091.14	10^{-4} in^{-1}
b_2	-13.752	4.072	10^{-4} in^{-2}
b_3	-1.415	3.429	10^{-4} in^{-3}
b_4	8.0	4.7	10^{-4} in^{-4}
b_5	.25	-.62	10^{-4} in^{-5}
b_6	-5.	-.82	10^{-4} in^{-6}

In Table VIII, a comparison of the measured values with the design is given for the quadrupole and sextupole terms.

Table VIII: Synchrotron standard magnet measured parameters[4]

Parameter	Positive (VF) wide-gap magnet DESIGN	Positive (VF) wide-gap magnet MEASURED	Negative(HF) narrow-gap magnet DESIGN	Negative(HF) narrow-gap magnet MEASURED	Unit
Gradient effective length	126.5	125.99	126.5	126.09	in
k_1	-.043508	-.0437352	.043622	.0435214	m^{-1}
k_2	-.0421376	-.04319	.029711	.012789	m^{-2}

The table shows that the as-built magnets have a larger VF gradient and a smaller HF gradient than the design; this will tend to increase the vertical tune and decrease the horizontal. The gradient lengths for both magnets are smaller than the design, which will tend to decrease both tunes. Although the sextupole in the VF magnet is close to the design, that in the HF magnet is too small by more than a factor of two; thus the horizontal chromaticity will not be fully corrected. As far as the higher harmonics go, inspection of Table VII shows that there is significant b_4 (decapole); however, given the short cycle time of the machine, this is probably of little practical significance.

B. Synchrotron Modified-Gradient Field Measurements

The modified magnets were measured and reported in [5]. Table IX summarizes the results. No attempt has been made to fit the measured fields at the same level of detail as was done for the main magnets. Instead, the ratio of the measured value of ξ_{00} to the design value has been used to scale the design value of x_0, to give a "measured" value, and Eq. (8) has then been used to obtain "measured" values of the focusing parameter k_1.

Table IX: Synchrotron modified magnet measured parameters[5]

Parameter	Positive (VF) wide-gap magnet	Negative(HF) narrow-gap magnet	Unit
Gradient effective length	125.97	126.16	in
ξ_{00} measured)	4.839	4.592	in
ξ_{00} design)	4.854	4.588	in
x_0 (design)	4.738	4.731	in
x_0 (measured)	4.7233	4.7351	in
k_1 (measured)	-.084446	.084235	m^{-2}
k_1 (design)	-.0839755	.0840998	m^{-2}

C. L0 and L3 matching quadrupoles

In the early 1970's, during the efforts to get the machine to the highest possible energy, the quadrupoles in the long straight sections were replaced. The lengths and focusing strengths of the new quadrupoles are reported in [6]. The separation of the doublet elements is taken from [7]; this has also been confirmed by direct measurement of the remaining doublet in L0. This information is presented in Table X.

Table X: Synchrotron L0, L3 new quadrupole parameters

Parameter	Quadrupole	Unit
Gradient length	.6373	m
Quadrupole focusing strength parameter k_Q	.40096	m^{-2}
Quadrupole spacing	.6716	m

D. As-built MAD Lattice

The measured values for the quadrupole and sextupole focusing strength parameters, and the measured gradient effective lengths, together with the information in Table X, have been used in the MAD lattice to obtain global lattice parameters corresponding to the "as-built" lattice. The results are given in Table XI.

Table XI: As-built lattice global parameters

Parameter	Horizontal	Vertical	Longitudinal	Units
Tune	10.642	10.8298		
Chromaticity	-10.95	3.408		
Momentum compaction			.0098216	
Circumference			755.8428	m
Beta(max)	22.87	22.68		m
Dispersion (max)	2.937	0.		

Table XII: Synchrotron standard magnet measured and fitted focusing strength parameters[4]

Parameter	Positive (VF) wide-gap magnet FITTED	Positive (VF) wide-gap magnet MEASURED	Negative(HF) narrow-gap magnet FITTED	Negative(HF) narrow-gap magnet MEASURED	Unit
k_1	-.0436437	-.0437352	.0435501	.0435214	m^{-1}
(Fitted-measured)/Measured)		0.21		0.07	%

The experimentally measured tunes are very sensitive to the values of the main magnet focusing strengths, and are probably the best determinants of these values. Because of this, I have tried to get better values for the focusing strengths by allowing them to vary to reproduce the measured high-energy tunes (Q_x=10.686, Q_y=10.819) in the current lattice. The model of the current lattice described below in section III was used for this exercise. Table XII gives the comparison between the focusing strengths so obtained and the measured strengths from Table VII. From [4], the quoted errors on the measured gradient lengths are 0.15%.

The fitted values for the main magnet focusing strength parameters from Table XII are then taken as the best estimates of these quantities and have been used in the "as-built" pre-CESR lattice to give the global lattice parameters displayed in Table XIII. The resulting pre-CESR lattice functions are plotted in fig. 7-9. Also plotted in Fig. 10 is the tune vs. momentum offset. The large negative value of the horizontal chromaticity is a result of the failure to meet the design specification for the sextupole term in the main HF magnet.

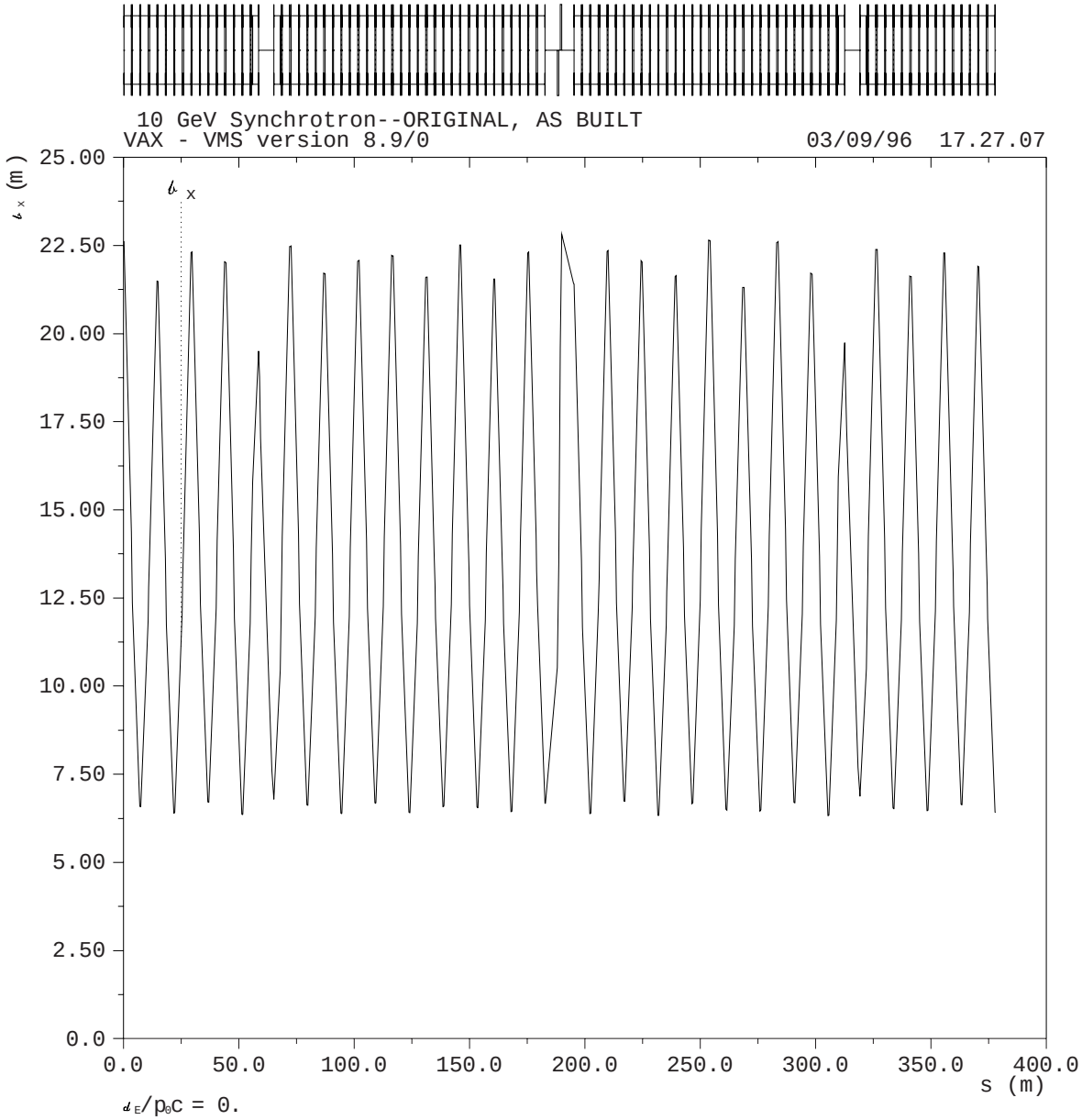

Fig 7.
As-built lattice: horizontal beta function
Half ring, Starting at table 144
in positron direction

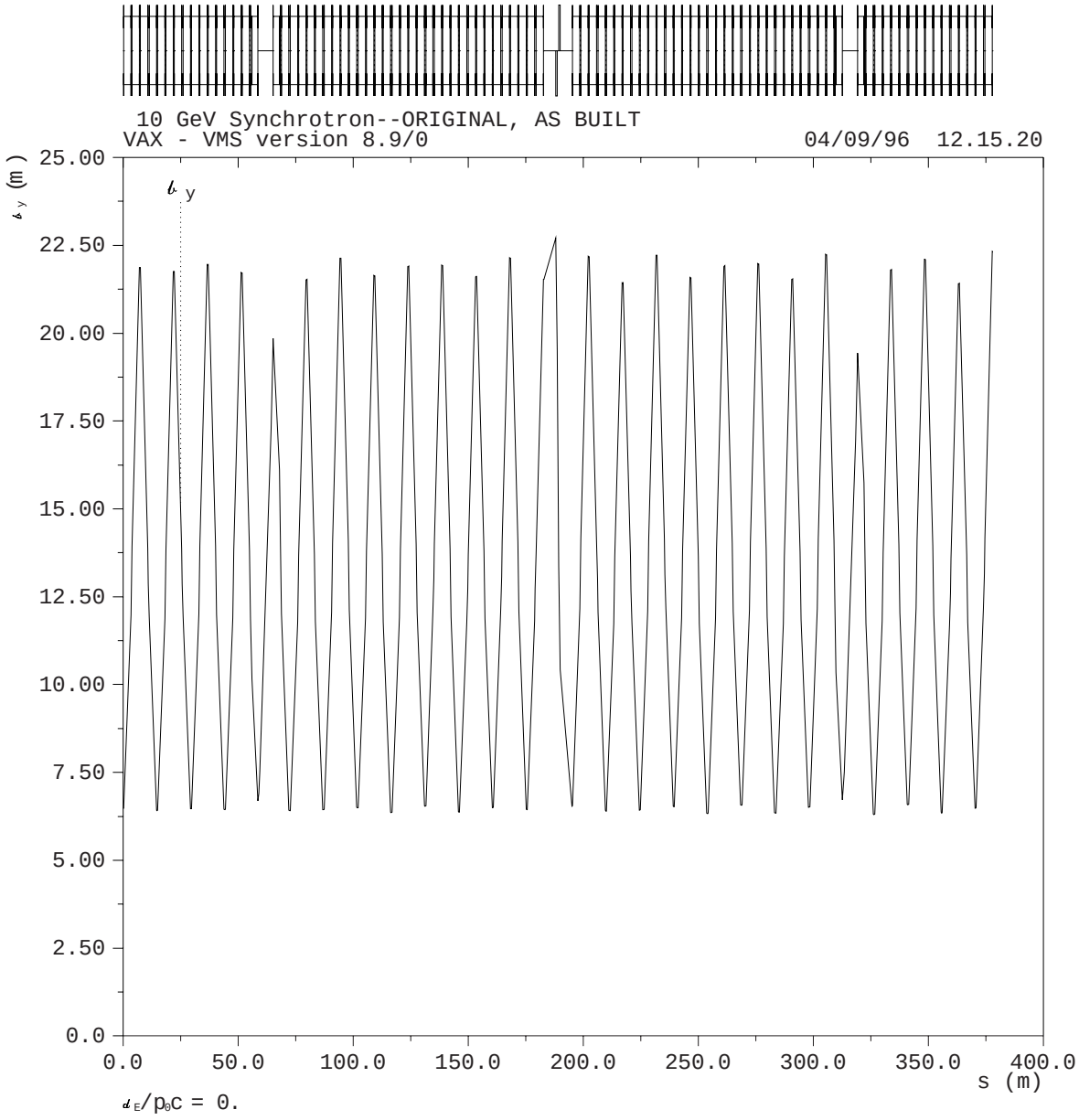

Fig. 8
As-built lattice: vertical beta function
Half ring, Starting at table 144
in positron direction

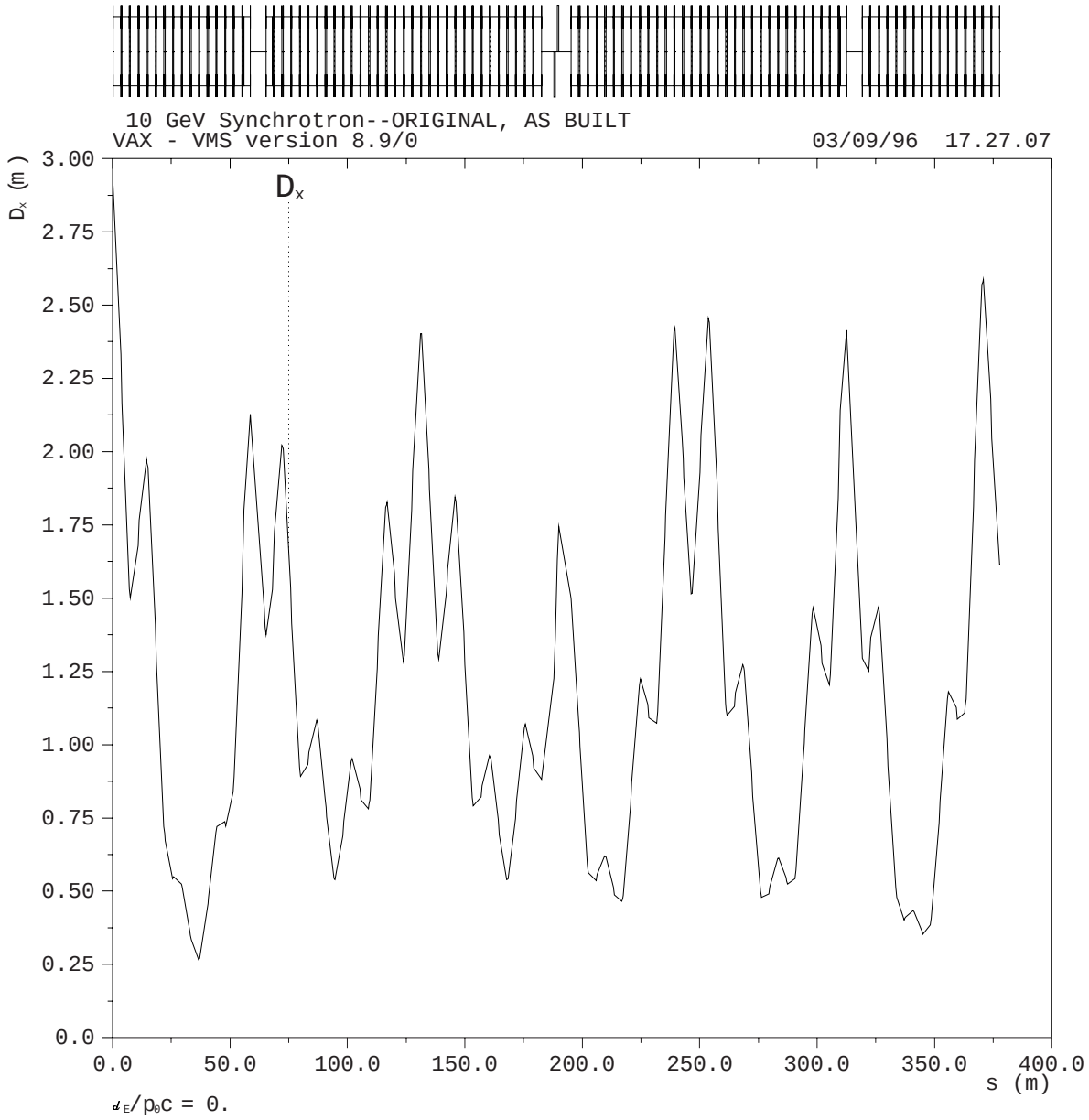

Fig. 9
As-built lattice: horizontal dispersion function
Half ring, Starting at table 144
in positron direction

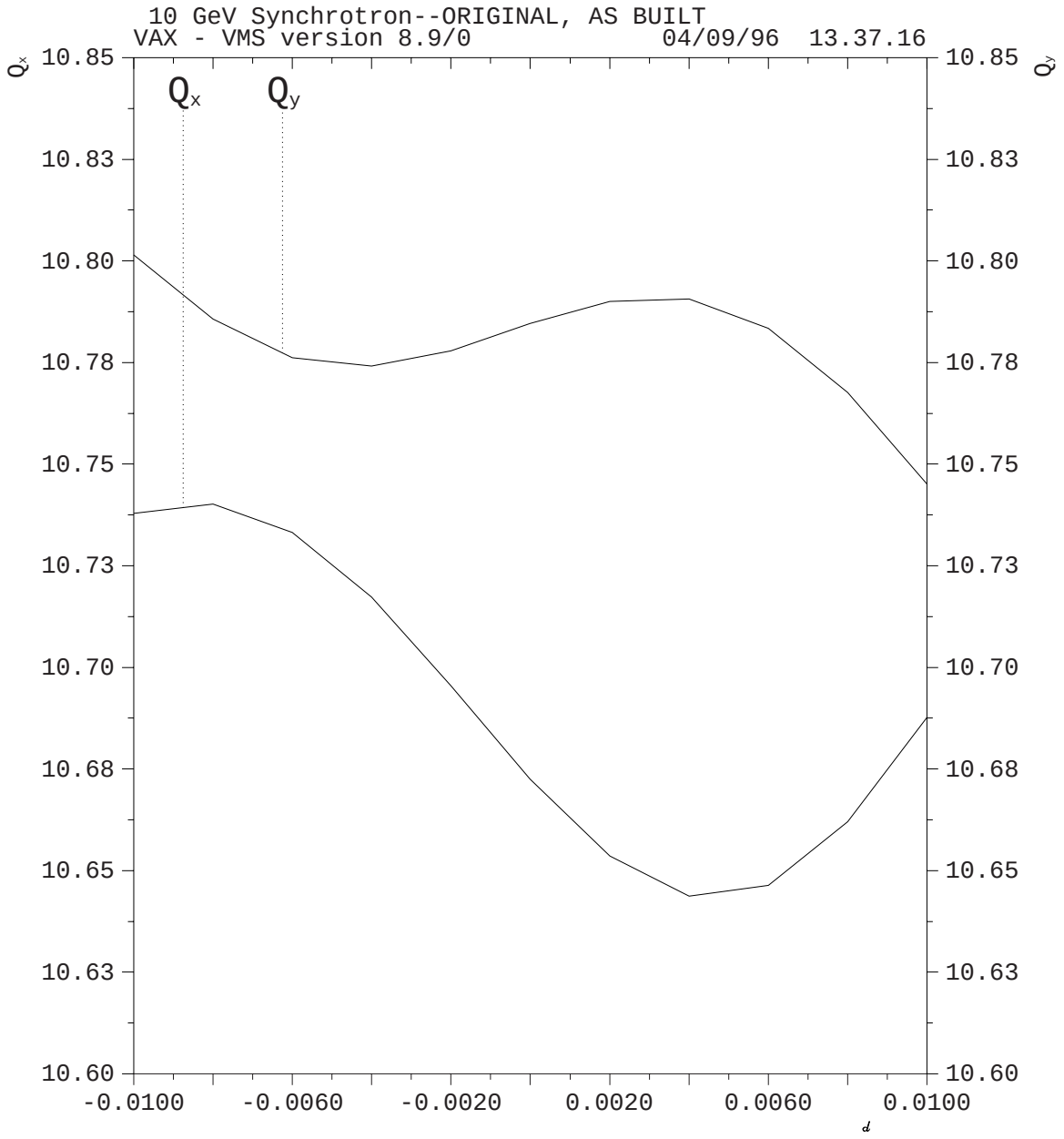

Fig. 10
As-built synchrotron lattice
Tune vs. momentum offset

Table XIII: As-built lattice global parameters;
with main magnet k_1's adjusted to give measured tunes in current lattice

Parameter	Horizontal	Vertical	Longitudinal	Units
Tune	10.672	10.784		
Chromaticity	-10.95	3.37		
Momentum compaction			.0097578	
Circumference			755.8428	m
Beta(max)	22.81	22.71		m
Dispersion (max)	2.91	0.		

G. Apertures and ideal machine acceptance

The horizontal good field regions quoted above in sec. II.A, together with the design location of the geometric centerline relative to the isomagnetic line, and the beam's sagitta relative to this line as expressed by Eqs. (12) and (13), can be combined to obtain the horizontal aperture for the beam in each type of magnet. The results are listed in Table XIV. The vertical apertures have been set equal to half the magnet gap.

Table XIV: Synchrotron magnet half-apertures

Parameter	Positive (VF) wide-gap magnet	Negative(HF) narrow-gap magnet	Unit
Horizontal aperture	1.98	2.5	cm
Vertical aperture	1.9	1.27	cm

With these apertures, one can evaluate the machine acceptance, as determined only by the principal magnets. I will call this the "ideal acceptance". The actual acceptance will always be less than this, of course, due to additional aperture restrictions, magnet placement errors, etc.

The ideal acceptance was calculated using the "as-built" pre-CESR lattice. In MAD, collimators were inserted at every magnet as specified in Table XIV. Particles of increasing betatron amplitude were tracked for 50 turns. The maximum betatron amplitude which survived, as a function of the momentum offset from the central momentum, was determined. This is a measure of the physical aperture of the machine. The result is shown in fig. 12. The betatron amplitudes have been converted into a phase space area, and this area/π is plotted as the acceptance in the figure. The ideal vertical acceptance is 11.5 μm-rad.

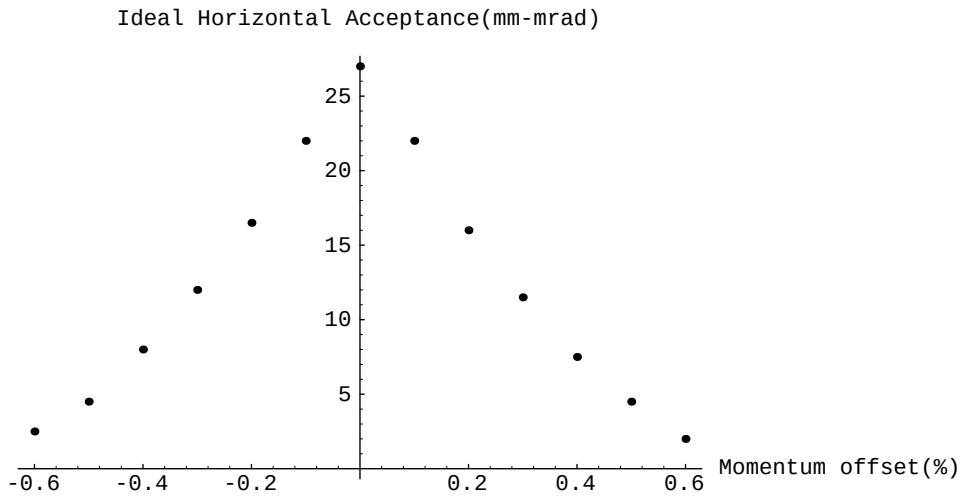

Fig. 12 Pre-CESR synchrotron ideal horizontal acceptance vs. momentum offset

III. CESR ERA MODIFICATIONS

A. Main Magnet Moves in L2 and L4 for Extraction to CESR

When CESR was installed, in order to accommodate the required transfers of electrons and positrons, extraction systems had to be installed in L2 and L4. To accommodate the septa and kickers into the synchrotron lattice, some of the main magnets were moved[6]. These moves caused a closed orbit distortion and introduced a lattice function mismatch. The closed orbit distortion outside of the region where the magnets were moved was minimized by a 0.106 in radial inward shift of the magnets[6]. Within the region of the magnet moves, there is a small shift (.54 cm) in the closed orbit from that of the unperturbed machine. The lattice function mismatch, of course, affects the entire machine.

In L4, magnets 141 and 140, 137 and 136, and 134 and 133 were each moved away from the other by 6.5 in, opening an additional 13 in of space for the insertion of septa and a kicker for positron extraction. In L2, magnets 58 and 57, 55 and 54, and 51 and 50 were moved in a similar way for electron extraction.

The pre-CESR MAD lattice described above in section II has been modified to reflect these changes. Table XV gives the global parameters of the new lattice.

Table XV: pre-CESR lattice global parameters;
with main magnet moves for extraction to CESR

Parameter	Horizontal	Vertical	Longitudinal	Units
Tune	10.649	10.774		
Chromaticity	-11.08	3.353		
Momentum compaction			.0098119	
Circumference			755.8428	m
Beta(max)	27.96	25.76		m
Dispersion (max)	3.15	0.		

Note that the peak beta functions have increased by 22%(x),14%(y) and the peak dispersion has increased by 8%, over the original machine. Fig. 12, 13 and 14 give plots of the lattice functions around the ring, which no longer has twofold antisymmetry.

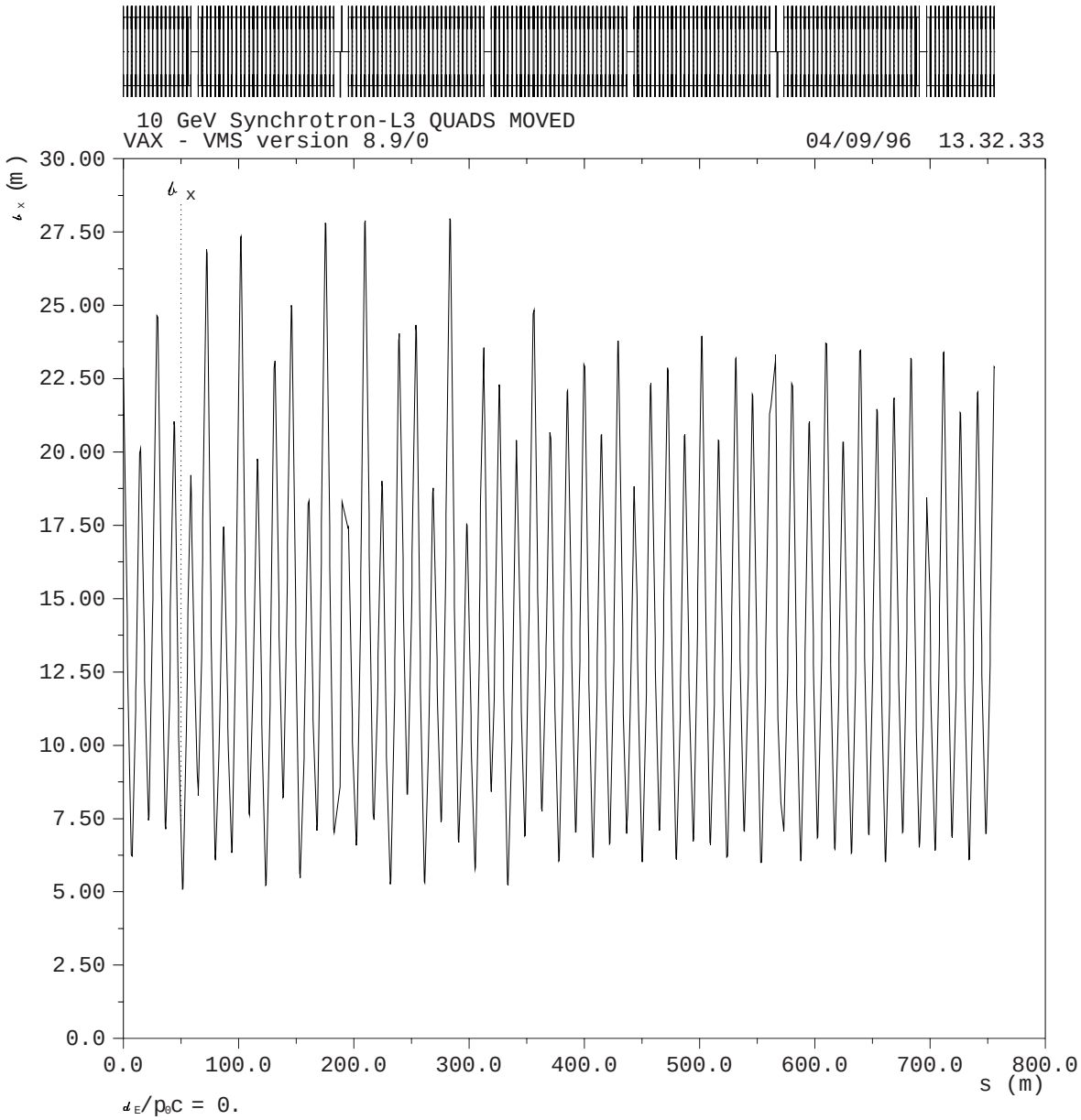

Fig 12: As-built lattice after magnet moves for CESR injection: horizontal beta function
Full ring, Starting at table 144, in positron direction

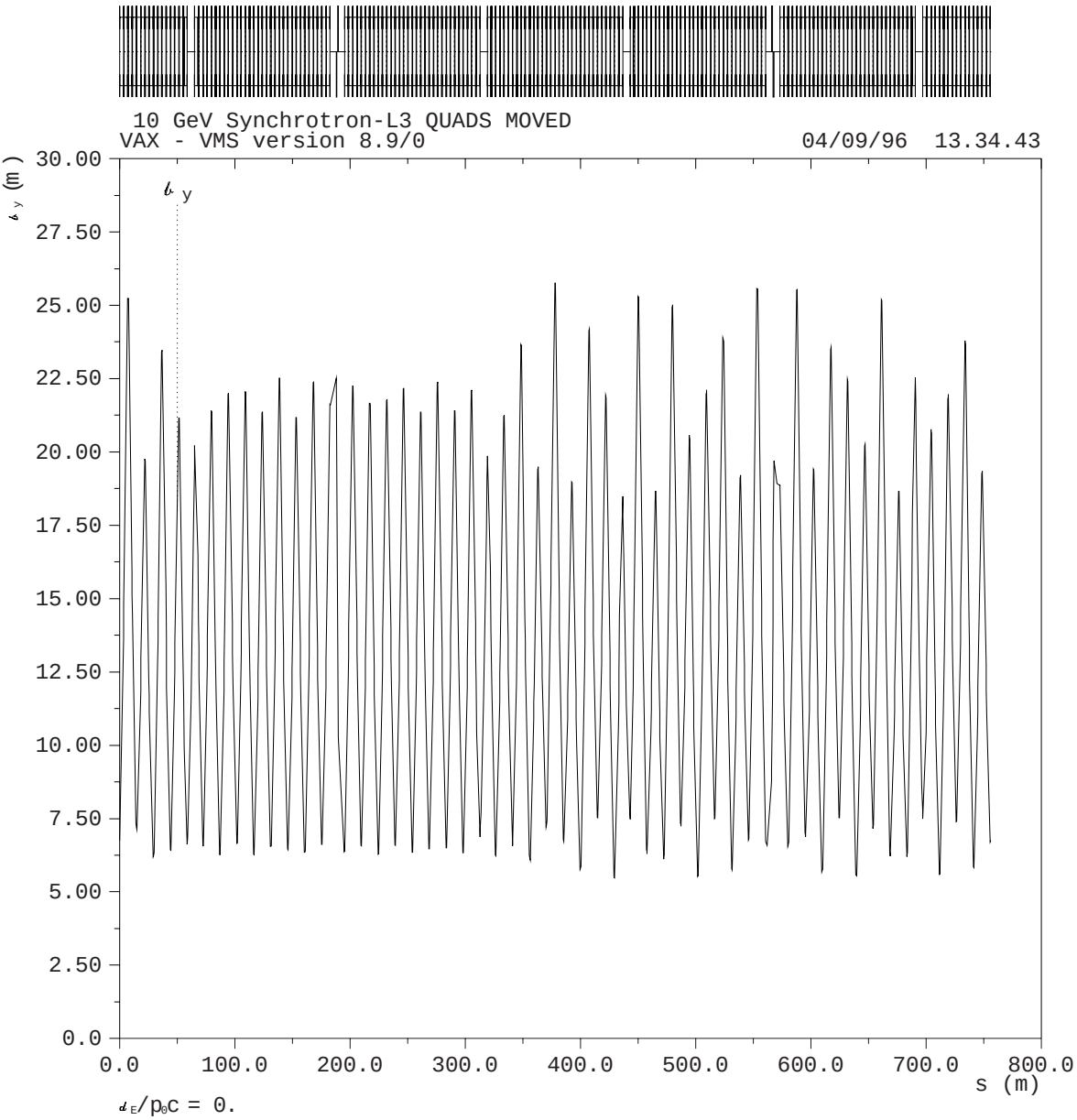

Fig 13: As-built lattice after magnet moves for CESR injection: vertical beta function
Full ring, Starting at table 144
in positron direction

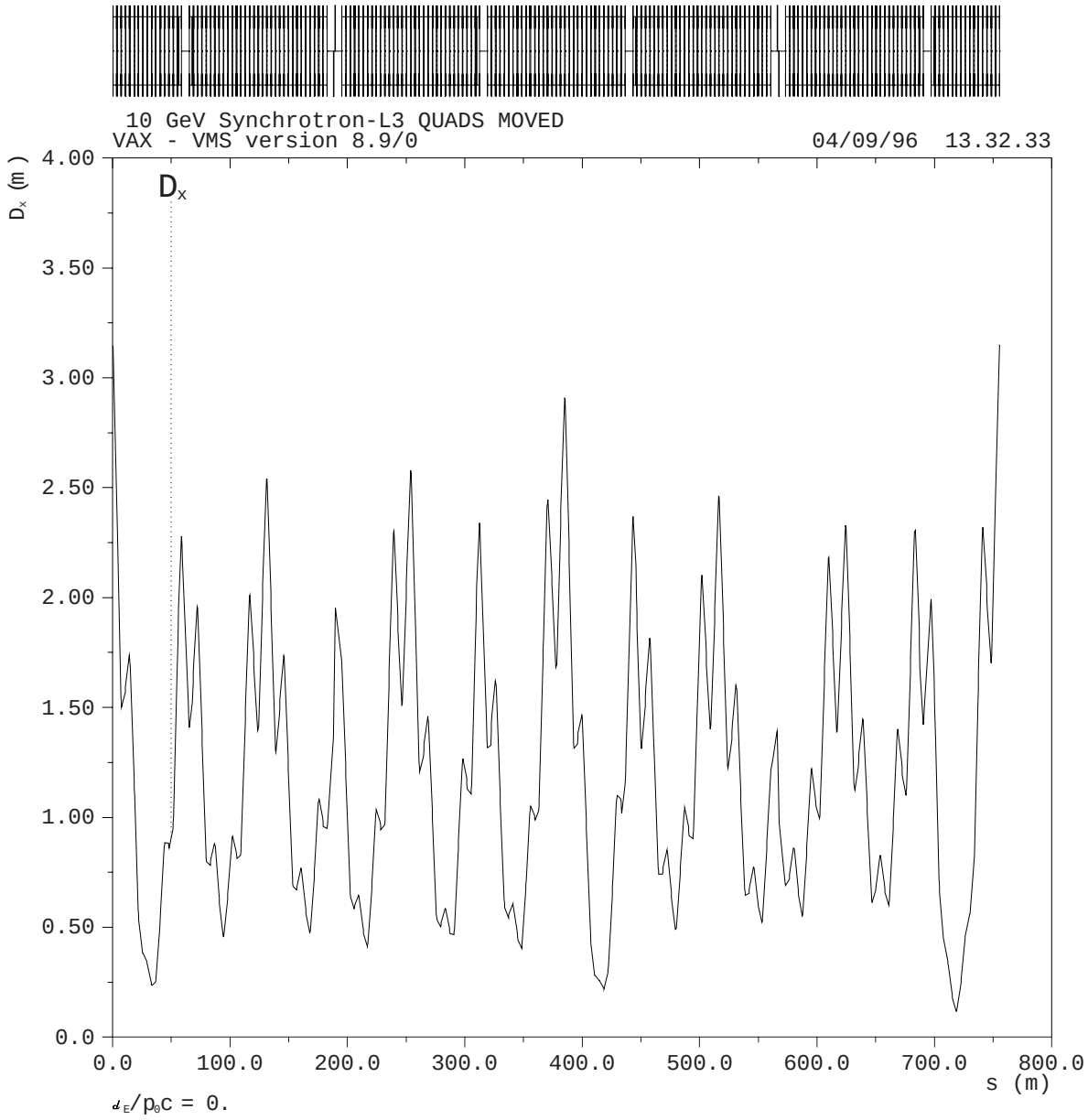

Fig 14:
As-built lattice after magnet moves for CESR injection: horizontal dispersion function
Full ring, Starting at table 144
in positron direction

The ideal horizontal acceptance of the new lattice is presented in Fig. 15. (The small effects of the radial magnet shifts on the effective horizontal apertures of the magnets which were moved in L2 and L4 have been ignored).The ideal vertical acceptance is 10 μm-rad Both acceptances are significantly reduced from that of the pre-CESR lattice because of the lattice function perturbations.

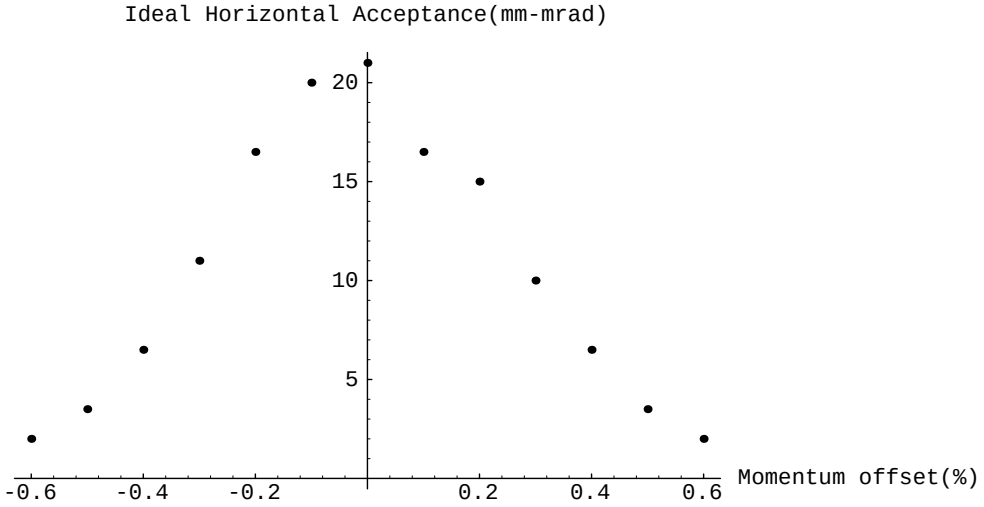

Fig. 15 Original as-built lattice with main magnet moves for extraction to CESR:
Ideal horizontal acceptance vs. momentum offset

B. Modifications in the L0 straight for positron injection,
and in the L0 sector for electron injection

An injection system for positrons was installed in L0 at the time of CESR construction. However, the system did not require the reconfiguration of any elements in the synchrotron. The aperture restrictions introduced by this system in the L0 straight (due to the septum and kicker) are not severe and have been ignored.

At the time of CESR construction, no changes were made in the electron injection lines. However, in the late 1980's, the electron injection line was reconfigured[7,8]. Although no synchrotron magnets were moved from their nominal longitudinal locations, the HF magnet M13 was replaced by a VF magnet, which was installed in this slot rotated by 180º about a vertical axis, so that it presents a HF gradient to the beam. The magnet used has a special lamination with a channel on the outside for an extracted beam, and was originally used at one of the machine's extraction points. After rotation by 180º, the channel is on the inside of the machine and facilitates electron injection when used at M13. This is, however, a wide-gap magnet and so has a slightly different gradient, a smaller horizontal aperture, and a larger vertical aperture, than a standard narrow-gap HF magnet. These small effects have not been included in the lattice or the ideal acceptance calculations presented here.

C. Modifications in L3

In order to accommodate plans for a detector in CESR in the north area, the quadrupole doublet in the center of L3 had to be removed. In its place, two quadrupole doublets were installed at either end of the L3 straight. These doublets, identical to the pair in L0 except for their relative separation, were intended to match across the L3 straight. The geometry of the doublet configuration is presented in Table XVI. The quadrupole spacings have been taken from [7] and also confirmed by direct measurement.

Table XVI: Synchrotron L3 quadrupole reconfiguration for CESR

Parameter	Quadrupole	Unit
Effective length	.6373	m
Quadrupole focusing strength parameter k_Q	.40096	m^{-2}
Quadrupole doublet spacing	.4620	m
Center of L3 to center of each doublet	4.9256	m

This arrangement does not match the lattice functions across the long straight as well as the single doublet at L0. For the specified gradient, length, and location given in Table XVI, the doublet separation would have to be reduced to 0.21 m to achieve a perfect beta match. This close spacing is essentially impossible to realize physically with the existing quadrupoles. Consequently, additional perturbations are introduced into the beta and dispersion functions. Table XVII presents the global parameters of the lattice with the L3 modification, which is essentially the current lattice.

Table XVII: Current lattice global parameters

Parameter	Horizontal	Vertical	Longitudinal	Units
Tune	10.686	10.819		
Chromaticity	-11.47	3.52		
Momentum compaction			.0097259	
Circumference			755.8428	m
Beta(max)	32.88	30.40		m
Dispersion (max)	3.54	0.		

The peak beta functions are now larger than in the original design by 44%(x), 34%(y), and the peak dispersion is greater by 22%. Fig. 16, 17 and 18 give plots of the lattice functions around the ring with the current lattice.

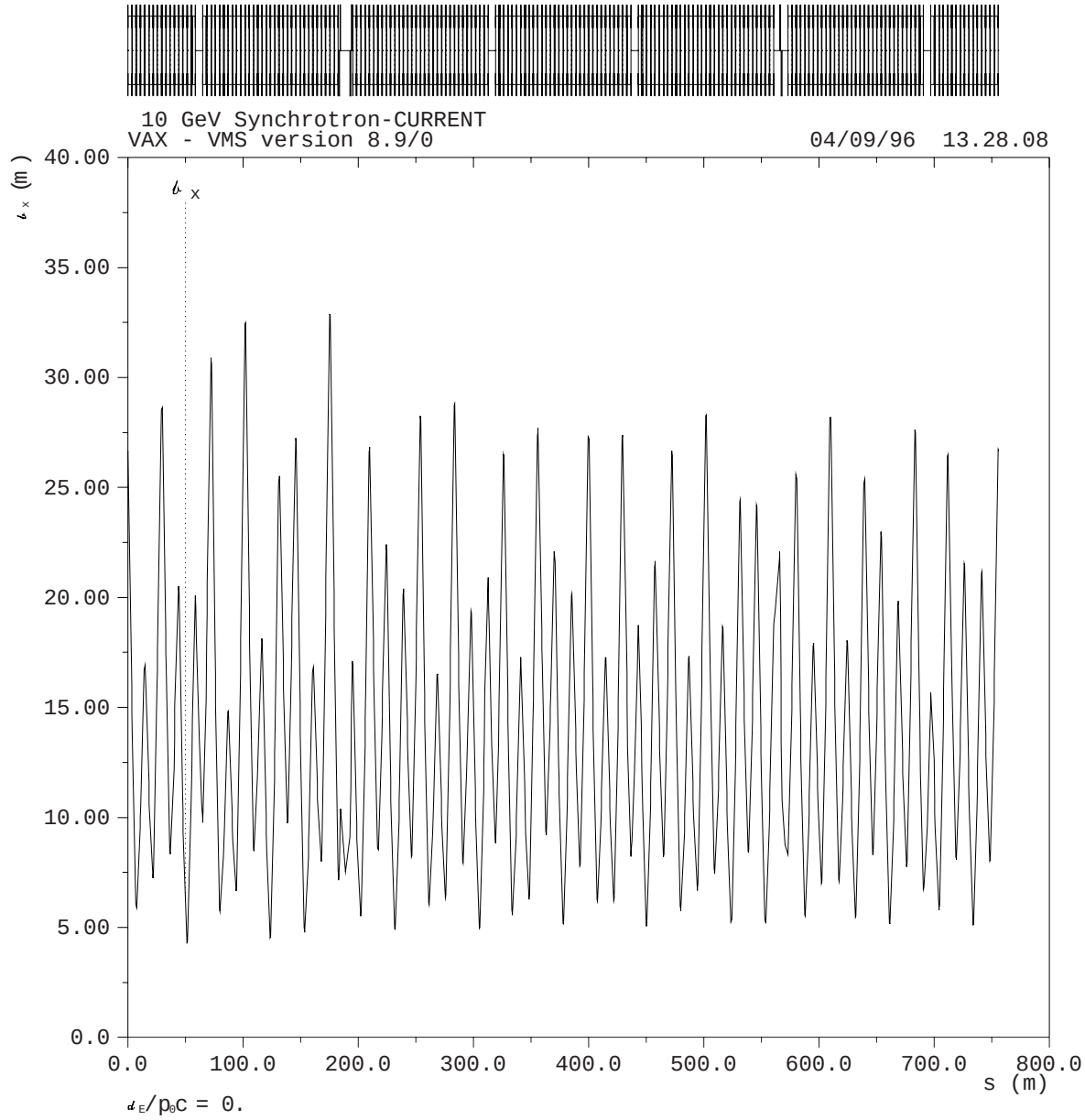

Fig 16:
Current lattice: horizontal beta function, full ring, starting at table 144, in positron direction

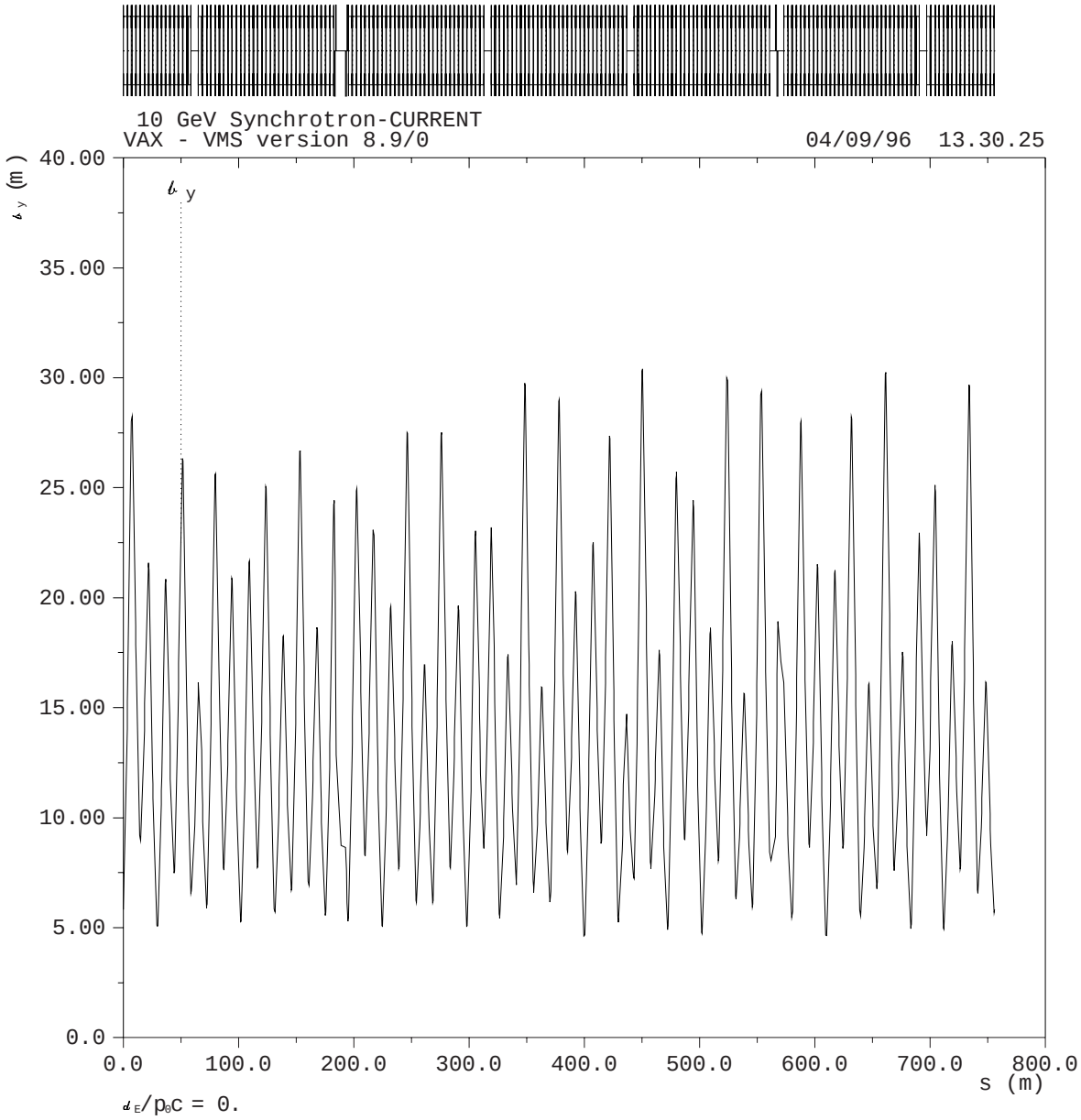

Fig 17:
Current lattice: vertical beta function
Full ring, Starting at table 144
in positron direction

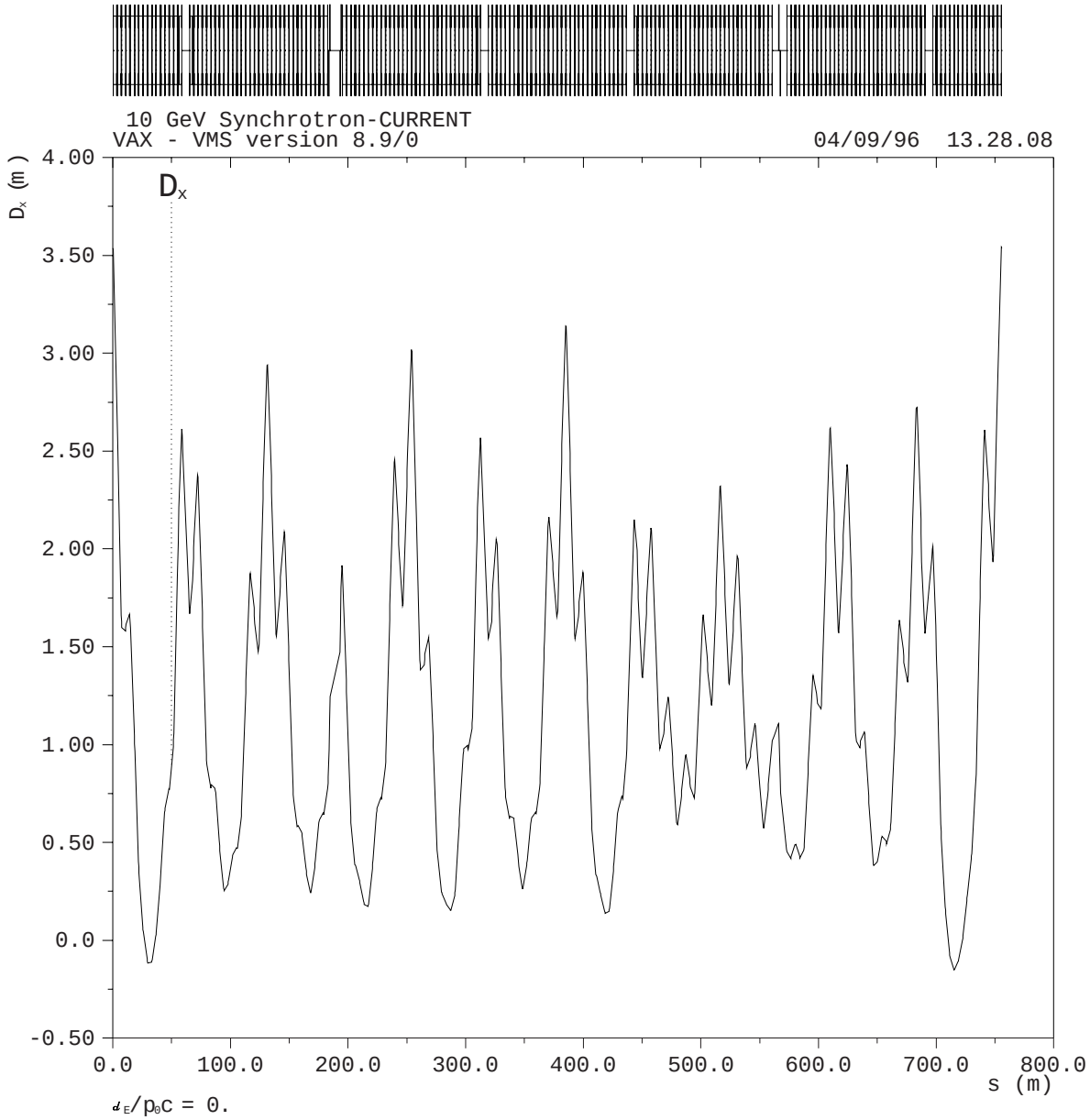

Fig 18:
Current lattice: horizontal dispersion function
Full ring, Starting at table 144
in positron direction

D. Ideal acceptance of the current machine

The ideal horizontal acceptance of the current lattice is presented in Fig. 19. The ideal vertical acceptance is 9 μm-rad. Both are significantly reduced from that of the pre-CESR lattice.

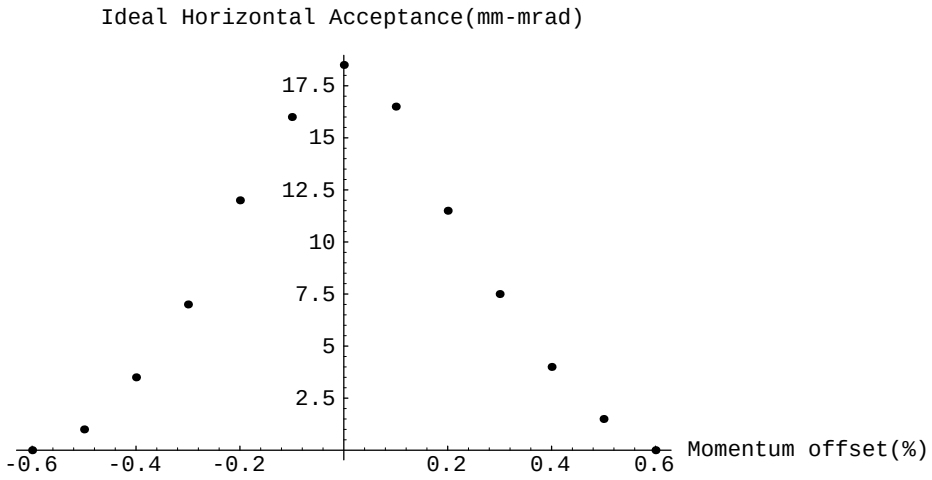

Fig. 19 Current lattice
Ideal horizontal acceptance vs. momentum offset

IV. PROPOSED RECONFIGURATION OF L3

Since there is no longer a detector in the north area of CESR, it is possible to reconfigure L3 back to the original design. In this case, the global lattice parameters should be those given in Table XV, with the lattice functions as shown in Fig. 12, 13 and 14. The peak beta functions should be reduced from the current lattice by 15% in x and 18% in y. The peak dispersion should be reduced by 12%. The tunes are shifted down by .038 in x and .044 in y. Fig. 20 shows a tune space plot of the current and reconfigured lattice tunes.

Resonances up to 4th order are shown. The new working point is a bit closer to the 3rd order fan from (.67,.67).

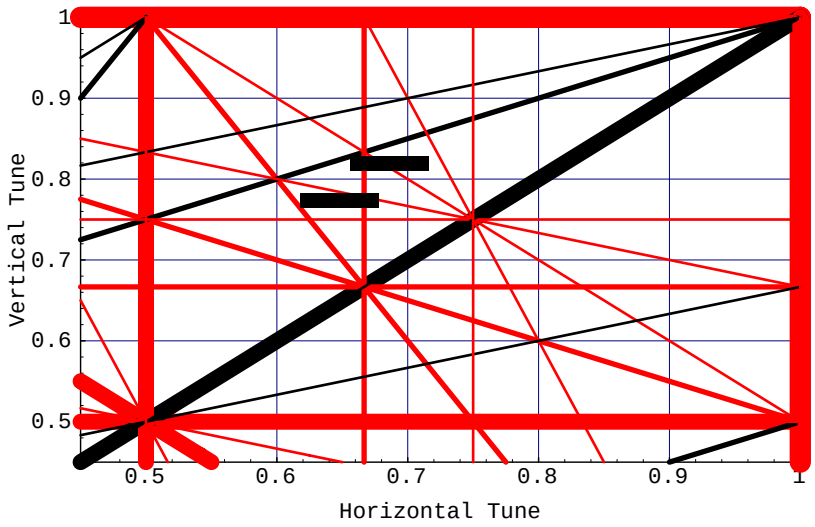

Fig. 20 Synchrotron tune space with resonance lines up to order 4

The current lattice is represented by the bar centered at (ν_x=.686, ν_y=.819),and L3-reconfigured lattice by that at (ν_x=.649, ν_y=.774). The length and width of the bars shows the chromatic tune spread due to a momentum width of +/-.3%.

The ideal acceptance is predicted to be that given in Fig. 15. Fig. 21 shows the ratio of the ideal acceptance with the reconfigured lattice to that of the current lattice. At large momentum offsets, gains in excess of 50% are predicted.

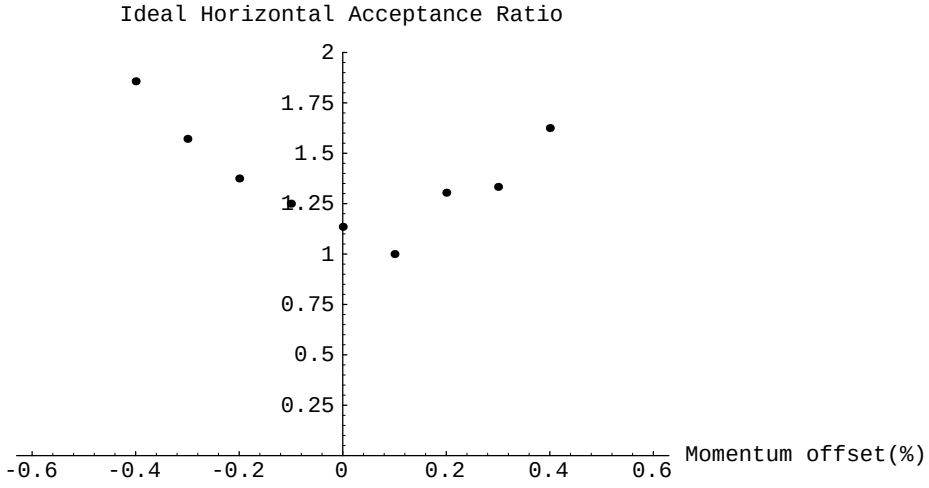

Fig. 21 Ratio of ideal horizontal acceptance of L3-reconfigured lattice to current lattice

V. REFERENCES

[1] R. R. Wilson, *The 10 to 20 GeV Cornell Electron Synchrotron*, CS-33 (1967)

[2] D. A. Edwards, *10 GeV Lattice II*, CSDS-25 (1965)

[3] P. N. Bredsen, P. C. Stein, *Pole Profiles of 10 GeV Bending Magnets*, CSDS-24 (1965)

[4] R. Yamada, S. Mori, *Magnetic Field Measurement I*, CS-31 (1966)

[5] R. Yamada, *Magnetic Field Measurement II*, CS-36 (1968)

[6] J. Seeman, *Injection Process of the Cornell Electron Storage Ring CESR*, (thesis, 1979)

[7]. G. Rouse, private communication

[8] E. Blum, *Synchrotron Injected Electron beam Trajectories*, CON 88-10(1988)